Calcium Ion Binding Properties and the Effect of Phosphorylation on the Intrinsically Disordered Starmaker Protein

ARTICLE *in* BIOCHEMISTRY · OCTOBER 2015

Impact Factor: 3.02 · DOI: 10.1021/acs.biochem.5b00933

6 AUTHORS, INCLUDING:

Magdalena Wojtas
Wroclaw University of Technology
7 PUBLICATIONS **31** CITATIONS
SEE PROFILE

Rafał Hołubowicz
Wroclaw University of Technology
1 PUBLICATION **1** CITATION
SEE PROFILE

Piotr Dobryszycki
Wroclaw University of Technology
39 PUBLICATIONS **229** CITATIONS
SEE PROFILE

BIOCHEMISTRY
including biophysical chemistry & molecular biology

Article

pubs.acs.org/biochemistry

Calcium Ion Binding Properties and the Effect of Phosphorylation on the Intrinsically Disordered Starmaker Protein

Magdalena Wojtas, Rafał Hołubowicz, Monika Poznar, Marta Maciejewska, Andrzej Ożyhar, and Piotr Dobryszycki*

Wrocław University of Technology, Faculty of Chemistry, Department of Biochemistry, Wybrzeże Wyspiańskiego 27, 50-370 Wrocław, Poland

ABSTRACT: Starmaker (Stm) is an intrinsically disordered protein (IDP) involved in otolith biomineralization in *Danio rerio*. Stm controls calcium carbonate crystal formation *in vivo* and *in vitro*. Phosphorylation of Stm affects its biomineralization properties. This study examined the effects of calcium ions and phosphorylation on the structure of Stm. We have shown that CK2 kinase phosphorylates 25 or 26 residues in Stm. Furthermore, we have demonstrated that Stm's affinity for calcium binding is dependent on its phosphorylation state. Phosphorylated Stm (StmP) has an estimated 30 ± 1 calcium binding sites per protein molecule with a dissociation constant (K_D) of 61 ± 4 μM, while the unphosphorylated protein has 28 ± 3 sites and a K_D of 210 ± 22 μM. Calcium ion binding induces a compaction of the Stm molecule, causing a significant decrease in its hydrodynamic radius and the formation of a secondary structure. The screening effect of Na^+ ions on calcium binding was also observed. Analysis of the hydrodynamic properties of Stm and StmP showed that Stm and StmP molecules adopt the structure of native coil-like proteins.

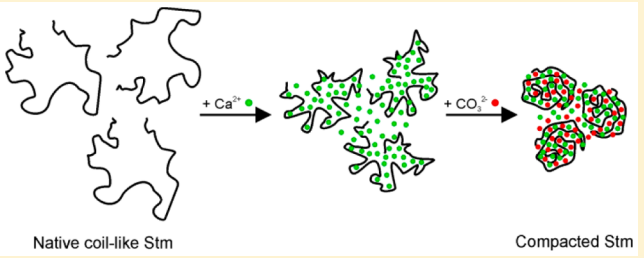

Biomineralization is a process of crystal formation under biological control. It involves selective uptake of metal ions and their incorporation into formed structures.[1] Biominerals are composite structures that fulfill various biological functions. Bones provide body support, protect organs, and are reservoirs of calcium and phosphate in vertebrates. Eggshells permit gas exchange and protect the embryo against damage and microbial infection. Many invertebrates, such as sea urchins, mollusks, and crustaceans, have developed exoskeletons or shells to protect their bodies from harsh environmental conditions or natural predators.[2] Otoliths in fish and otoconia in land vertebrates are involved in the sensing of linear acceleration.[3] Fish otoliths are also involved in sound detection.[4]

Biominerals differ significantly from inorganic crystals. They are often harder yet more flexible than a purely inorganic mineral. This is due to the organic macromolecules, mainly proteins, that strictly control biomineral formation.[5,6]

The final size, shape, polymorph, and hierarchical structure of a biomineral require a set of interactions between organic macromolecules and the inorganic phase such as calcium phosphate and calcium carbonate, which are abundant in nature. Insoluble matrix macromolecules, e.g., collagen and chitin, form a framework for mineral deposition, while the soluble fraction controls crystal growth.[7] This fraction is composed mostly of highly negatively charged acidic proteins.[8,9] They undergo extensive post-translational modifications[10,11] and frequently belong to the group of intrinsically disordered proteins (IDPs).[12] IDPs are dynamic, flexible, heterogeneous populations of molecules without a well-defined folded structure. Their highly charged character, along with the low content of hydrophobic amino acid residues, results in strong electrostatic repulsion and the lack of a well-packed hydrophobic core.[13] The high content of acidic groups in the proteins involved in biomineralization results in a greatly increased capability for binding calcium. It has been proposed that carboxyl or phosphate groups bind Ca^{2+} in the IDP bovine dentin phosphophoryn, a protein involved in the deposition of hydroxyapatite crystals during dentin mineralization.[14−16]

Other well-characterized calcium binding proteins such as calsequestrin, calreticulin, calnexin, and dehydrin-like have been previously described.[15,17−20] These proteins can bind from 10 to hundreds of calcium ions with varying affinity, mostly in the micromolar range of the dissociation constant. Protein phosphorylation enhances calcium ion binding and has a significant impact on protein folding and signaling pathways.[21,22]

Otoliths are biomineral structures composed of calcium carbonate and an organic matrix arranged in layers. They are situated in the inner ear of fish and are responsible for the reception of linear acceleration and gravity.[3,23] One of the best-studied proteins that control otolith formation is Starmaker (Stm) from *Danio rerio*. The *stm* gene was discovered by searching zebrafish cDNA libraries for *dspp*-like genes.[24] DSPP (dentin sialophosphoprotein) is a protein involved in tooth formation. It is proteolitically processed into DPP (dentin

Received: May 11, 2015
Revised: October 1, 2015
Published: October 6, 2015

DOI: 10.1021/acs.biochem.5b00933
Biochemistry 2015, 54, 6525−6534

phosphoprotein or phosphophoryn) and DSP (dentin sialoprotein).[25] Despite their relatively low level of sequence homology, Stm and DSPP seem to have analogous functions. Stm, like DSP and DPP, is a highly acidic protein rich in aspartyl (25%) and glutamyl (11%) residues, which might allow Stm to bind a large number of calcium ions. It was previously shown that Stm is an IDP with an extended, rodlike shape. It undergoes compaction in the presence of positively charged ions, mainly Ca^{2+}.[26,27] However, it is not known whether the compaction is caused by the formation of a more ordered secondary structure. Stm, which is an otolith component, controls biomineral size, shape, and polymorph *in vivo*.[24] It has been shown that reduction of Stm activity in zebrafish changes the crystal morphology and switches the polymorph from aragonite to calcite.[24] *In vitro* studies of Stm's influence on calcium carbonate crystal growth showed that Stm induced nucleation and then inhibited further crystal growth.[28] Moreover, in the presence of Stm, a polymer-induced liquid precursor (PILP) was observed.[28,29] PILP is a fluidic, amorphous phase of calcium carbonate that is formed in the presence of a negatively charged polymer.[28,29]

It was previously shown that Stm was phosphorylated *in vitro* by casein kinase 2 (CK2) and that this modification enhanced Stm biomineralization activity *in vitro*.[28] However, until now, no study of the amount of phosphorylated residues in the Stm sequence or the effect of phosphorylation on Stm conformation has been conducted.

The aim of this study was to determine the effect of the phosphorylation of Stm by CK2 on the structure and calcium binding properties of Stm. We conclude that the intrinsically disordered character of the Stm protein and its calcium binding properties may be crucial for biomineralization functioning.

MATERIALS AND METHODS

Buffers. The following buffers were used in the preparation of the protein and for the experiments: MOPS buffer [10 mM MOPS and 100 mM KCl (pH 7.2)], TG buffer [10 mM Tris and 10% (v/v) glycerol (pH 7.0)], and TNaG buffer [10 mM Tris-HCl, 100 mM NaCl, and 10% (v/v) glycerol (pH 7.0)].

Protein Preparation. The Stm protein was obtained as previously described.[27] Briefly, Stm was overexpressed in BL21(DE3)pLysS *Escherichia coli* cells and purified using fractionation with ammonium sulfate, size-exclusion chromatography, and hydroxyapatite chromatography. The concentration of Stm and StmP was measured using a Lowry assay with ovalbumin (OVA) as the standard.[30]

Protein Phosphorylation. The Stm protein was phosphorylated using casein kinase 2 (CK2) (Jena Biosceince, PR-314). A 0.5 M ATP stock solution was adjusted to pH 7.0 by adding a 2 M NaOH solution. The ATP:NaOH molar ratio in the final stock solution was 1:2. The reaction was conducted in a TG buffer supplemented with 10 mM $MgCl_2$ and different ATP concentrations (0 μM, 5 μM, 50 μM, 0.5 mM, 5 mM, and 50 mM). The Stm concentration in the reaction mixture was 0.5 mg/mL (7.7 μM); 66 milliunits of CK2 was used per milligram of protein. The mixture was incubated at 37 °C for 1.5 h. The phosphorylated protein was purified via gel filtration on a Superdex 200 10/300 GL column connected to the ÄktaExplorer system, equilibrated with a TG buffer.

Sodium Dodecyl Sulfate−Polyacrylamide Gel Electrophoresis (SDS−PAGE) with a Phos Tag. SDS−PAGE was performed according to the Laemmli protocol;[31] however, the resolving gel contained an additional 100 μM $MnCl_2$ and the Phos tag (NARD Institute, Ltd.). The acrylamide concentrations in the stacking and resolving gels were 4 and 10%, respectively.

Mass Spectrometry (MS). Before MS, 30−100 μg of Stm or StmP was purified by reverse phase chromatography and lyophilized. MS spectra were recorded with a MALDI-TOF apparatus (Autolflex II, Bruker Daltonics). Lyophilized Stm was diluted in 50 μL of Milli-Q water. A sample containing 0.5 μL of the Stm solution and 0.5 μL of a matrix [sinapinic acid diluted in a 50:50 (v/v) water/acetonitrile mixture, with 0.1% (v/v) TFA] was put on an MTPAnchorChip 384 T F instrument (BukerDaltonics). The mass spectrometer was calibrated with Protein Standard II (Buker Daltonics). Positively charged ions were registered in the range of 20000−100000 Da. Data were analyzed with FlexAnalysis version 2.2. The number of phosphate residues per protein molecule was estimated by subtracting the theoretical mass of the unphosphorylated protein from the experimentally determined mass of StmP, and then the difference was divided by the phosphate group mass (79 Da) and rounded to an integer.

Calcium Affinity Assay. The Rhod-5N fluorescent probe (Life Technologies) was used to measure the affinity of Stm and StmP for Ca^{2+}. A similar test using a different probe (Quin-2) was described by Engel et al.[32] The concentration of Stm/StmP in the samples was 4.0 μM. The fluorescence of the reference and the protein samples was measured at 22 ± 0.5 °C using a Fluorolog-SPEX fluorometer (Horiba, Jobin-Yvon). After Stm and StmP were incubated with Ca^{2+} for at least 30 min, 10 μL of 40 μM Rhod-5N in a TG buffer was added to a final volume of 200 μL. After incubation for 5 min, the excitation wavelength was set at 551 nm and emission was scanned between 560 and 600 nm at a rate of 1 nm/s. The minimal fluorescence (F_{MIN}) was measured using a sample containing 10 mM EDTA in a TG buffer; the maximal fluorescence (F_{MAX}) was measured for a protein-free sample saturated with 20 mM Ca^{2+}. All measurements were repeated in triplicate, each time using 60 μL of the assay mixture. Calculations were based on the fluorescence intensity at the emission maximum.

Reference samples were used to calculate the affinity of Rhod-5N for calcium ions using an approach suggested by McNamara et al.[33] The affinity of Stm and StmP for Ca^{2+} was calculated using an approach suggested by Linse et al.[34] with modifications. $K_{D,Stm}$ (the apparent dissociation constant) and n (the number of binding sites) were randomly set, initially between 0 and 10 mM for $K_{D,Stm}$ and 0−200 for n. For each $[Ca]_T$, the Newton−Raphson method was used to calculate free Ca^{2+} ($[Ca]_F$) with the equation

$$[Ca]_{T,i} = [Ca]_{F,i} + [Ca]_{B,Rhod,i} + [Ca]_{B,Stm,i} \quad (1)$$

where:

$$[Ca]_{B,Rhod,i} = ([Rhod][Ca]_{F,i})/(K_{D,Rhod} + [Ca]_{F,i})$$

and

$$[Ca]_{B,Stm,i} = (n[Stm][Ca]_{F,i})/(K_{D,Stm} + [Ca]_{F,i})$$

Calculated $[Ca]_{F,i}$ values were used to calculate $F_{T,i}$ (the theoretical fluorescence intensities if randomly selected $K_{D,Stm}$ and n were true):

$$F_{T,i} = F_{MIN} + (F_{MAX} - F_{MIN})([Ca]_{F,i})/(K_{D,Rhod} + [Ca]_{F,i}) \quad (2)$$

DOI: 10.1021/acs.biochem.5b00933
Biochemistry 2015, 54, 6525−6534

The accuracy of the fit was estimated by calculating the sum of squares of residuals:

$$\chi^2 = \sum_{i=1}^{n} [(F_{T,i} - F_i)/F_{MAX}]^2 \quad (3)$$

After 200000 estimations, 200 sets of $K_{D,Stm}$ and n with the lowest χ^2 were used to select new ranges for randomly setting these values. Calculations were finished when the set of the 200 best fitting values contained single values of $K_{D,Stm}$ and n. Statistical analysis was performed using a t test.

Traces of Ca^{2+}, possibly bound to Stm and StmP, were removed by incubation with 10 mM EDTA for 3 h on ice. EDTA was then removed by exhaustive dialysis against the TG buffer, which had been previously treated with Chelex 100 to remove trace calcium ions. After the last step of dialysis, the buffer was collected for use as a reference. The calcium concentration in the stock solution was measured using a QuantiChrom Calcium Assay Kit (BioAssay Systems).

Estimation of the Hydrodynamic Radius of the Protein. The hydrodynamic radius of the protein was estimated using size-exclusion chromatography as described previously.[35] The column was equilibrated with a TNaG or TG buffer; 100 μL of the 0.4 mg/mL protein was loaded onto a Superdex 200 10/300 GL column (Amersham Biosciences) connected to an ÄKTA explorer system (Amersham Biosciences). Chromatography was performed at room temperature using a flow rate of 0.5 mL/min. The column was calibrated with the following standard proteins: cytochrome c (17 Å), myoglobin (20 Å), ovalbumin (30.5 Å), bovine serum albumin (BSA) (37 Å), apoferritin (67 Å), and thyroglobulin (85 Å). The elution volume of each standard protein was used to calculate K_{AV} factors, which were then plotted against the corresponding Stokes radii.[36] The standard curve was used to calculate the Stokes radius of Stm and StmP in 5 μM, 50 μM, 1 mM, 10 mM, 20 mM, 50 mM, and 100 mM Ca^{2+}, as well as in the absence of Ca^{2+}. Theoretical values of the Stokes radius that were expected for fully unfolded, fully folded, and partially folded conformations of the globular protein with a corresponding molecular mass were estimated from the following empirical equations (eqs 4–9).[37]

$$\log(R_S^N) = -(0.204 \pm 0.023) + (0.357 \pm 0.005) \times \log(M) \quad (4)$$

$$\log(R_S^{MG}) = -(0.053 \pm 0.094) + (0.334 \pm 0.021) \times \log(M) \quad (5)$$

$$\log(R_S^{PMG}) = -(0.21 \pm 0.18) + (0.392 \pm 0.041) \times \log(M) \quad (6)$$

$$\log[R_S^{U(GdmCl)}] = -(0.723 \pm 0.033) + (0.543 \pm 0.007) \times \log(M) \quad (7)$$

$$\log[R_S^{NU(coil)}] = -(0.551 \pm 0.032) + (0.493 \pm 0.008) \times \log(M) \quad (8)$$

$$\log[R_S^{NU(PMG)}] = -(0.239 \pm 0.055) + (0.403 \pm 0.012) \times \log(M) \quad (9)$$

where M = 64497 Da (the molecular mass of Stm) and N represents the native form, MG represents the molten globule, PMG represents the premolten globule, U(GdmCl) represents the globular protein unfolded by GdmCl, and NU(coil) and NU(PMG) represent the natively unfolded protein having a coil-like and pre-molten globule-like conformation, respectively.

Sedimentation Velocity (SV) Ultracentrifugation. The sedimentation velocity experiment was performed using a Beckman Coulter ProteomeLab XL-I ultracentrifuge (version 6.0, Beckman Coulter Inc.) and an An-60Ti rotor. Cells with sector-shaped two-channel charcoal-filled Epon centerpieces were used. Sample sectors were filled with 400 μL of 0.2 mg/mL Stm or StmP in 10 mM Tris (pH 7.0) supplemented with 100 mM NaCl, 100 mM $CaCl_2$, or both. The experiment was conducted overnight at 50000 rpm in 20 °C. Cells were scanned for absorbance at 230 nm.

Data analysis was performed using SEDFIT (available at http://www.analyticalultracentrifugation.com/). Scans representing the whole sedimentation process were selected for data analysis. The density and dynamic viscosity of solvents and the partial specific volume of Stm at 20 °C were estimated using SEDNTERP (available at http://sednterp.unh.edu/[38]). Timestamp correction was applied using a function implemented in SEDFIT.[39] A continuous $c(s)$ distribution model was used to estimate sedimentation coefficients (s) and frictional ratios (f/f_0). Data were fitted to 250 points from 0 to 25 S. Standardized sedimentation coefficients ($s_{20,W}$), hydrodynamic radii (R_H), and the apparent molecular weight of Stm were also calculated. Maximal entropy regularization with p = 0.68 was applied.[40]

Circular Dichroism (CD) Spectroscopy. CD spectra for Stm and StmP in the presence of calcium ions (0, 1, and 100 mM) were recorded with a Jasco J-815 spectropolarimeter equipped with a temperature control unit (Jasco CDF-426S). Measurements were performed at 20 °C with 0.4–1 mg/mL solutions of protein in a TG buffer. Samples were measured in 100QS cuvettes (Hellma) with a path length of 0.2 mm. The spectra were recorded in a spectral range of 190–260 nm with a 1 nm bandwidth, an integration time of 1 s, a data pitch of 1 nm, and a scan speed of 50 nm/min. Each spectrum represents the average of five scans. Three independent experiments were performed for each CD analysis. The contribution of the TG buffer was subtracted from the original data, which were then converted to the mean molar residue ellipticity. CD spectra were analyzed with CDPro (http://lamar.colostate.edu/~sreeram/CDPro/main.html) to estimate the secondary structure composition of the protein. Calculations were made using a CONTINLL algorithm by comparing the spectrum to the spectra from the SDP48 basis.[41]

RESULTS

Phosphorylation of Stm Protein.[42,43] Phosphorylation is an essential modification for many of the proteins responsible for crystal formation.[10] They are frequently phosphorylated by protein kinases, such as casein kinase 2 (CK2), which recognize acidic consensus sequences.[42,43] Stm phosphorylated by CK2 exhibits greater biomineralization activity, so it is important to know how many phosphate groups are introduced by CK2.[28] We investigated the phosphorylation of Stm by CK2 kinase and determined that the phosphorylation level strongly depended on the concentration of ATP (Figure 1).

StmP with different numbers of phosphate groups was analyzed via SDS–PAGE. The resolving gel was modified with

DOI: 10.1021/acs.biochem.5b00933
Biochemistry 2015, 54, 6525–6534

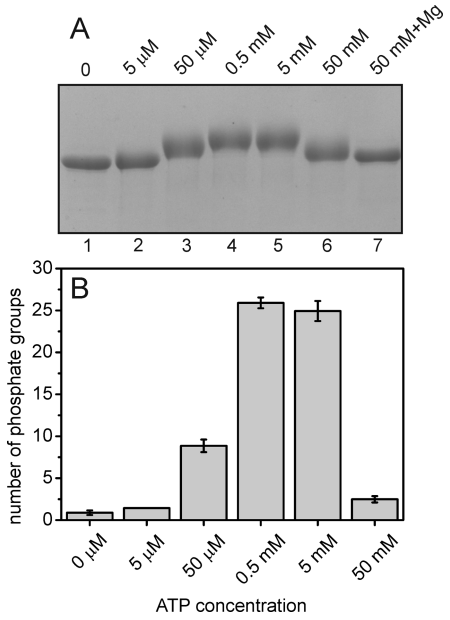

Figure 1. Phosphorylation of Stm. Stm was phosphorylated with CK2 at several ATP concentrations. (A) SDS−PAGE analysis of StmP. The resolving gel was prepared with 100 μM Phos tag. The ATP concentration in the phosphorylation mixture is indicated above the gel. (B) Number of phosphate groups per protein molecule estimated by mass spectrometry.

a Phos tag, which is a manganese complex that specifically interacts with phosphate groups in proteins. It decreases the electrophoretic mobility of phosphorylated proteins, in contrast to that of unphosphorylated proteins, thus making it possible to visualize the degree of phosphorylation[44,45] (Figure 1A). We observed different levels of Stm phosphorylation depending on the ATP concentration in the solution. The largest shift in Stm mobility was observed when ATP concentrations in the reaction mixture were 0.5 and 5 mM. MS analysis showed that CK2 phosphorylates 2−26 Ser/Thr residues per protein molecule, depending on the ATP concentration (Figure 1B and Table 1). Surprisingly, at 50 mM ATP, only two phosphate groups were introduced into Stm. We checked to see if this was caused by an insufficient concentration of Mg^{2+}. Because 50 mM ATP and 10 mM $MgCl_2$ were present, only part of the ATP should have formed a complex with the ions. However, an increase in the $MgCl_2$ concentration to 100 mM did not increase the level of phosphorylation of Stm (Figure 1A, line 7).

Table 1. Molecular Masses of Stm and StmP Obtained by MS

[ATP]	mass determined by MS (Da)	mass difference (Da)	no. of phosphate groups per protein	theoretical mass[a] (Da)
0 mM	64567.1 ± 60.2	70.1	0	64497.0
5 μM	64610.7[b]	113.7	1	64610.6
50 μM	65196.9 ± 59.1	699.9	9	65196.3
0.5 mM	66543.5 ± 50.8	2046.5	26	66541.8
5 mM	66466.7 ± 94.3	1969.7	25	66465.1
50 mM	64693.4 ± 29.9	196.4	2	64693.2

[a]The theoretical mass of Stm was estimated by ProtParam (http://web.expasy.org/protparam/), while the theoretical mass of StmP was calculated by adding the mass of the phosphate groups (the number of phosphate groups estimated with MS; 79 Da each) to the theoretical mass of unphosphorylated Stm. [b]The result obtained from one measurement.

Stm Is a Calcium Binding Protein. Many proteins involved in the biomineralization of calcium carbonate and calcium phosphate bind calcium ions.[16,46,47] We determined that Stm is a calcium binding protein by using a quantitative calcium affinity assay[32] based on the competition between Stm and the fluorescent probe sensitive to calcium ions (Rhod-5N) (Figure 2).

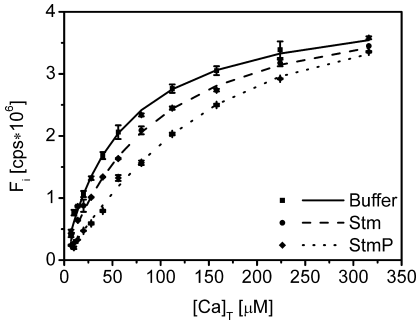

Figure 2. Calcium affinity of Stm and StmP. Fluorescence intensity measured at 575 nm for Rhod-5N alone (■), Rhod-5N with Stm (●), and Rhod-5N with StmP (◆). The calibration curve for Rhod-5N is a black line; the calcium binding fit for Stm is a dashed line, and the calcium binding fit for StmP is a dotted line. All measurements were made in triplicate.

Calcium binding by Stm and StmP was observed as a Rhod-5N fluorescence signal in samples containing Stm and StmP lower than that in the control samples (Figure 2). Fluorescence intensities were used to calculate the affinity of Stm and StmP for Ca^{2+}. The results are summarized in Table 2.

Table 2. Calcium Binding Properties of Stm and StmP[a]

	$K_{D,Stm}$ (μM)	n	χ^2
Stm	210 ± 22	28 ± 3	0.0058
StmP	61 ± 4	30 ± 1	0.0027

[a]$K_{D,Stm}$, dissociation constant; n, number of binding sites; χ^2, sum of squares of residuals.

The results of the calcium binding assay showed that Stm bound 28 calcium ions per molecule with an apparent K_D of 210 μM. StmP bound 30 calcium ions per molecule with an apparent K_D of 61 μM. Although the increase in the number of calcium binding sites caused by phosphorylation is not statistically significant ($p > 0.05$), the dissociation constant decreased significantly ($p < 0.001$). This suggests that phosphorylation facilitates binding of calcium ions by Stm.

Stm Conformational Change in the Presence of Ca^{2+}. It was previously shown that Stm undergoes compaction in the presence of Ca^{2+}, Mg^{2+}, or Na^+ ions. The decrease in the protein hydrodynamic radius is the largest in the presence of Ca^{2+}.[26] Phosphorylation has also been shown to increase the biomineralization activity of Stm *in vitro*.[28] Because StmP binds calcium ions more strongly than Stm, we made a comparison of the conformation of Stm and StmP in the presence of Ca^{2+} using gel filtration, sedimentation velocity analytical ultracentrifugation, and CD spectroscopy. Calcium ions caused a decrease in the hydrodynamic radius of both StmP and Stm (Figure 3). The gel filtration experiment was performed in two

DOI: 10.1021/acs.biochem.5b00933
Biochemistry 2015, 54, 6525−6534

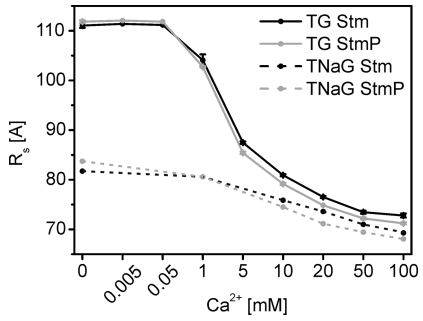

Figure 3. Effect of Ca^{2+} on the hydrodynamic radii of Stm and StmP. The R_S values estimated from analytical gel filtration obtained for Stm (black lines) and StmP (gray lines) in a TNaG buffer (dashed lines) and in a TG buffer (solid lines).

different buffers: a TNaG buffer (containing 100 mM NaCl) and TG (no salt). The proteins reached a similar degree of compaction with high concentrations of Ca^{2+} in both buffers (approximately 70−75 Å), but their hydrodynamic radius in the TG buffer was significantly higher at low concentrations of Ca^{2+} (~110 Å) compared to the measurement performed in TNaG (~83 Å). In TG, the total change in the Stm/StmP Stokes radius was ~40 Å, while in the TNaG buffer, it was ~13 Å (Figure 3). This was due to the lack of counterions in the TG buffer, which would have decreased the degree of intramolecular electrostatic repulsion of Stm and StmP. A comparison of the Stokes radii of Stm and StmP indicated that both proteins are similarly extended in the absence of Ca^{2+}, while at higher ion concentrations, they become compacted. This effect was observed in both buffers (Figure 3).

A sedimentation velocity experiment was conducted to validate results obtained from gel filtration (Figure 4 and Table 3). It was also used to check for the presence of aggregates that could be formed by protein in solution with Ca^{2+}. The $c(s)$ distribution contains strong signals at 2.5−3.5 S, which correspond to Stm and StmP. In contrast to gel filtration, sedimentation velocity reveals that structures of Stm and StmP are different, as suggested by the difference in the frictional ratio. Comparison of $s_{20,W}$ values allows us to conclude that StmP sediments faster than Stm and that calcium ions cause a significant increase in the sedimentation coefficients of Stm and StmP. An increase in the sedimentation coefficient is not caused by an increase in mass, but by compaction of Stm and StmP, which is reflected by a large decrease in frictional ratios and hydrodynamic radii, and by a negligible change in the estimated molecular weights. These results confirm that the decrease in the hydrodynamic radius of Stm and StmP in the presence of calcium is caused by compaction of the molecule rather than by dissociation of the subunits.

All the values obtained from the gel filtration and sedimentation velocity experiments were far from the results expected for globular proteins and their partially folded forms (Figure 5 and Tables 3 and 4). Even in the presence of 100 mM Ca^{2+}, the value of the Stm Stokes radius was similar to that for native coil-like proteins. As observed previously, frictional ratio values (f/f_0) estimated from the sedimentation velocity experiment (2.2−3.1) are also far greater than the value typical for folded proteins.[26] For BSA, the molecular weight of which is close to that of Stm and StmP, f/f_0 = 1.35.[48]

Interestingly, for ≤1 mM calcium ion, we observed the strong influence of NaCl on the hydrodynamic radius of Stm and StmP. Repulsion forces between negatively charged acidic side chains of Stm and StmP were neutralized by pairing sodium ions with charged carboxyl groups. Calcium ions coordinated by carboxyl groups probably replaced sodium ions, causing the further compaction of Stm and StmP.

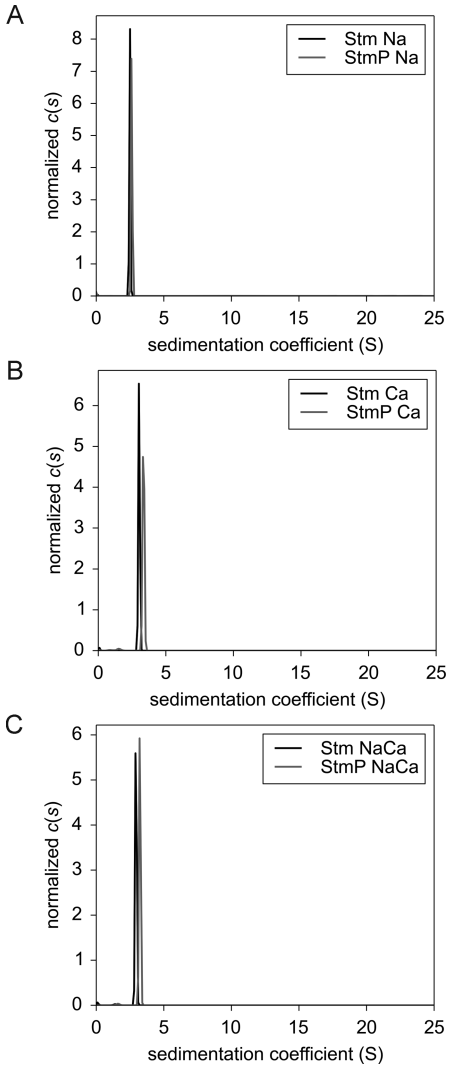

Figure 4. $c(s)$ distributions of Stm and StmP. $c(s)$ distributions of Stm (black lines) and StmP (gray lines) in 10 mM Tris (pH 7.0) supplemented with (A) 100 mM NaCl, (B) 100 mM $CaCl_2$, and (C) 100 mM NaCl and 100 mM $CaCl_2$.

Table 3. Parameters Derived from the Sedimentation Velocity Experiment[a]

	sample	s	$s_{20,W}$	f/f_0	MW (kDa)	R_S (Å)
Stm	100 mM NaCl	2.499	2.552	3.111	74.0	84.0
	100 mM $CaCl_2$	3.028	3.171	2.552	76.2	69.6
	100 mM NaCl and 100 mM $CaCl_2$	2.945	3.141	2.537	74.4	68.6
StmP	100 mM NaCl	2.628	2.684	2.992	75.3	81.3
	100 mM $CaCl_2$	3.351	3.351	2.284	75.1	62.0
	100 mM NaCl and 100 mM $CaCl_2$	3.237	3.237	2.317	74.9	62.8

[a] s, sedimentation coefficient; $s_{20,W}$, sedimentation coefficient standardized for water at 20 °C; f/f_0, frictional ratio; MW, fitted molecular weight; R_S, hydrodynamic radius.

DOI: 10.1021/acs.biochem.5b00933
Biochemistry 2015, 54, 6525−6534

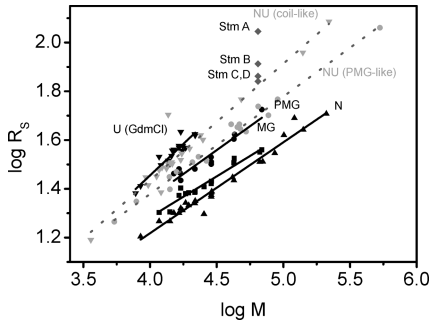

Figure 5. Dependence of the logarithm of the hydrodynamic radius (R_S) on the logarithm of the molecular mass for globular proteins (solid line) and IDPs (dashed line). Globular proteins and IDPs are marked with black and gray markers, respectively: N, native (triangles); MG, molten globule (squares); PMG, premolten globule (circles); U, unfolded by 6 M GdmCl (reversed triangles); NU, natively unfolded proteins. Data are taken from refs 37 and 49. Dark gray diamonds represent data experimentally obtained for Stm under different experimental conditions (named as indicated in Table 3).

Table 4. Comparison of Experimentally Obtained Stokes Radii of Stm with Calculated Values

		experimental values[a]	
protein	name	buffer	R_S (Å)
Stm	Stm_A	TG	111.1
	Stm_B	TNaG	81.7
	Stm_C	TG and 100 mM $CaCl_2$	72.8
	Stm_D	TNaG and 100 mM $CaCl_2$	69.3
StmP	StmP_A	TG	111.8
	StmP_B	TNaG	83.7
	StmP_C	TG and 100 mM $CaCl_2$	71.2
	StmP_D	TNaG and 100 mM $CaCl_2$	68.1
		theoretical values[b]	
		conformation	R_S (Å)
N		native	32.58 ± 3.53
MG		molten globule	35.76 ± 16.06
PMG		premolten globule	47.40 ± 41.13
U (GdmCl)		unfolded	77.37 ± 11.88
NU (coil-like)		native	66.09 ± 10.72
NU (PMG-like)		native	50.03 ± 12.98

[a]Obtained using gel filtration. [b]Calculated according to Uversky.[37]

Influence of Calcium on the Secondary Structure of Stm and StmP. The relative changes in the dimensions of Stm and StmP induced by Ca^{2+} are significant. A small difference in the conformation of Stm and StmP was also observed. Gel filtration and sedimentation velocity did not provide any information about secondary structures; therefore, we used circular dichroism (CD) spectroscopy to compare the secondary structure of Stm and StmP in the presence of calcium ions (Figure 6). A TG buffer was used for CD measurements.

The CD spectra of Stm and StmP exhibited shapes typical for IDPs. There was a large minimum near 200 nm, which is characteristic for unfolded proteins.[50] A comparison of the CD spectra of Stm and StmP shows that phosphorylation induced a slight change in the secondary structure (Figure 6). In the absence of metal ions, StmP was slightly more disordered than Stm. The higher negative charge of StmP resulted in stronger intramolecular electrostatic repulsion and a slightly less ordered secondary structure.

Although a significant change in the Stm and StmP hydrodynamic radius in the presence of Ca^{2+} was observed, the calcium ions induced only a small change in the secondary structures (Figure 6). Quantitative analysis of the spectra of Stm and StmP with CDPro revealed that 100 mM calcium ions caused a slight decrease in the disordered structure content, compensated mostly by an increase in the content of turns and β-sheets (Figure 6, insets). This was slightly more pronounced in StmP than in Stm, but the proteins remained disordered (~70% of the sequence). The conformational change induced by the calcium ions led to an increase in the level of ordered secondary structure of ~10% for StmP and even less for Stm.

DISCUSSION

Proteins involved in the control of biomineral formation are often intrinsically disordered. Included in these are the SIBLING proteins (small integrin binding ligand and N-linked glycoprotein), which are responsible for hydroxyapatite mineralization in vertebrates.[51] They control the formation of bone (bone sialoprotein, BSP; osteopontin, OPN)[52,53] and teeth (DSP, DPP, dentin matrix protein, DMP1).[54,55] The flexibility and extension of BSP are advantageous to the way it functions in cell attachment to the hydroxyapatite in bone.[56] The disordered structure of DPP supports extension across the surfaces of the hydroxyapatite crystals with a smaller number of DPP molecules that are able to cover the same area than in the

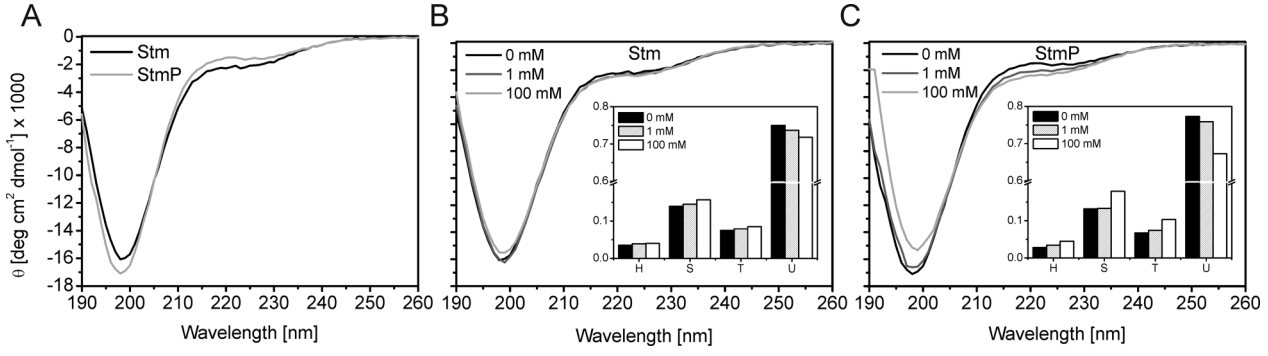

Figure 6. Effect of Ca^{2+} on the Stm and StmP secondary structure. (A) CD spectra of Stm (black) and StmP (gray). (B and C) CD spectra of Stm and StmP, respectively, in the presence of various Ca^{2+} concentrations: 0 mM (black), 1 mM (gray), and 100 mM (light gray). CDPro software was used to analyze the secondary structure content. In the insets, the secondary structure fraction is plotted vs the secondary structure type. H, α-helical structure; S, β-strands; T, turns; U, unstructured.

DOI: 10.1021/acs.biochem.5b00933
Biochemistry 2015, 54, 6525−6534

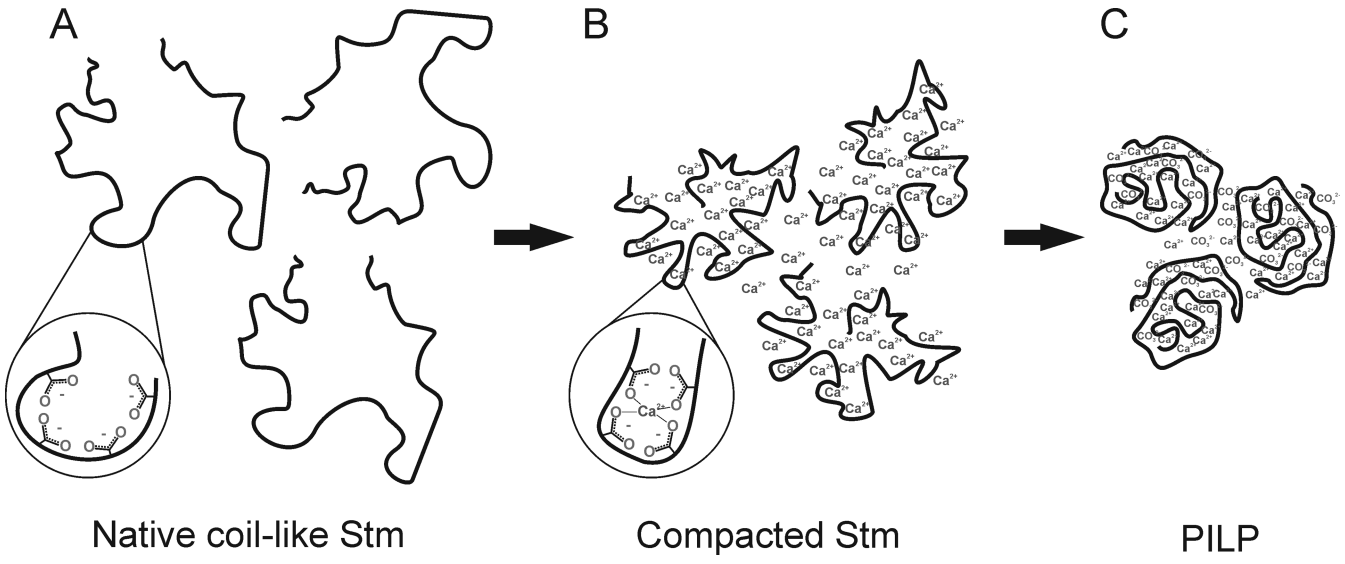

Figure 7. Proposed model of the compaction of the Stm molecule that leads to PILP formation. (A) Stm extended in the absence of calcium ions at low ionic strengths. (B) Calcium ions bind to the protein carboxyl and phosphate groups. The ionic interactions trigger compaction of the Stm molecule. (C) PILP is formed and subsequently transforms into calcite crystals.

case of a globular protein. This results in an inhibitory effect on crystal growth.[57] There are several other invertebrate proteins, which are also IDPs, involved in biomineralization.[12] AP7, AP24, lustrin A and asprich from mollusk shells, and CAP-1 from crustaceans are members of the IDP family.[58−63] The examples mentioned here strongly confirm the significance of disordered protein structure in biomineralization activity.

Proteins involved in biomineralization are often highly phosphorylated.[10] The disordered nature of Stm facilitates phosphorylation and calcium binding. Interestingly, we observed a different level of Stm phosphorylation that was highly dependent on the ATP concentration in the solution. There are 104 putative phosphorylation sites in the Stm sequence that were predicted for CK2. The Stm concentration in the reaction mixture was 7.7 μM. Assuming a 100% yield of phosphorylation, an average of 6.5 sites per Stm molecule would be phosphorylated with 50 μM ATP (concentration recommended by the CK2 supplier). In contrast, an ATP concentration from 0.5 to 5 mM would allow for the theoretical introduction of up to 650 phosphate groups into the Stm molecule. An ATP concentration from 0.5 to 5 mM is also much closer to the physiological level.[66] Surprisingly, the Stm phosphorylation level with 50 mM ATP was lower than for 5 mM ATP. Monovalent ions have been shown to decrease the activity of CK2.[64,65] With 50 mM ATP, the concentration of sodium ions was ∼100 mM, because the ATP stock was prepared with the addition of NaOH (see Materials and Methods). Because the ATP concentration in a cell ranges from ∼1 to 5 mM,[64,65] we believe that under physiological conditions Stm might be phosphorylated in at least 20−30 positions. The phosphorylation level could be even higher, because the ATP concentration is roughly constant in a cell, and also other kinases that recognize motifs other than CK2 could be involved in the phosphorylation of Stm. To confirm such a hypothesis, Stm isolated from otoliths would have to be tested.

We found that Stm bound ∼30 calcium ions per molecule. Although no canonical calcium binding motifs are present in the Stm sequence, there is a characteristic fragment rich in alternating D and S residues (D-rich region).[24] We conclude that abundant acidic residues are engaged in calcium binding like in calsequestrin or proteins from the S100 family.[67,68] The extension and flexibility of the Stm molecule might have additionally enhanced the calcium binding capacity, because most of the amino acid residues were exposed to the solvent and consequently were more accessible for ion binding than what would have been for a well-folded, globular protein.

A previously described qualitative radioisotope calcium binding test for phosphophoryn showed that phosphorylation had a strong impact on phosphophoryn calcium binding properties.[16] In a similar dot blot test with[45] Ca^{2+}, no such difference was observed between Stm and StmP (not shown). However, in our research, phosphorylation was observed to increase the affinity of Stm for calcium ions, as shown by the decrease in the apparent K_D from 210 to 61 μM. Calcium binding proteins often bind calcium with a K_D of from 10 to 1000 μM.[15,17−20] Interestingly, fish endolymph contains a concentration of calcium ions from 1.0 to 1.3 mM;[69,70] therefore, in its native state, StmP should be saturated with calcium. The phosphorylation-induced increase in the affinity for calcium binding may be what is crucial for the biomineralization of otoliths, because phosphorylation may facilitate a local increase in the concentration of calcium ions leading to the creation of PILP.

Gel filtration of Stm and StmP has suggested that phosphorylation may affect Stm's structure and modulate a conformational change in the presence of calcium ions. Sedimentation velocity has further supported these observations. As in phosphophoryn, which is a functional analogue of Stm, the conformation of the protein is more strongly affected by Ca^{2+} when the protein is phosphorylated.[16] Calcium ions appear to reduce the level of electrostatic repulsion of the Stm and StmP molecule, which leads to compaction of the protein, yet the molecule remains mostly disordered. Analysis of the hydrodynamic properties of Stm and StmP showed that even at 100 mM Ca^{2+}, Stm and StmP adopted the structure of a native coil-like protein (Figure 5). This supports the conclusion that compaction of the Stm molecule is not the result of a major disorder-to-order transition. We believe that the compaction of the Stm molecule is crucial for the formation of calcium

DOI: 10.1021/acs.biochem.5b00933
Biochemistry 2015, 54, 6525−6534

carbonate crystals in otolith biomineralization. Previous research showed that in the presence of a polyanion, PILP might be formed at the beginning of the crystallization process, meaning that in the presence of ions an acidic protein stabilizes a hydrated liquid phase precursor that accumulates and takes on variable shapes as an amorphous solid; this then subsequently transforms into a crystal.[29,71] We previously observed that Stm formed PILP during *in vitro* biomineralization.[28] Stm is extended in the absence of calcium ions, especially at low ionic strengths. The addition of Ca^{2+} to the solution resulted in the compaction of the Stm molecule, which may have led to sequestration and concentration of the ionic species. Consequently, more nucleation sites were created, and PILP was formed, which was subsequently transformed into calcite crystals. Such a mode of action may have an additional advantage. Even with a high concentration of calcium ions, the crystallization process would not be rapid. This is important because biological fluids, including the inner ear endolymph of teleosts, are supersaturated with calcium ions.[69,70] A proposed model of PILP formation is presented in Figure 7. Interestingly, calcium ions are not the only ions that affect the conformation of Stm. Compaction of Stm was previously observed in the presence of Na^+, K^+, Ca^{2+}, and Mg^{2+}.[26] Calcium ions caused the greatest decrease in the Stokes radius, while sodium ions had the smallest impact. In a TG buffer, the Stm Stokes radius was ∼111 Å, while in the same buffer supplemented with 100 mM NaCl, the Stokes radius was 82 Å. The presence of calcium caused further compaction of Stm to a radius of ∼70 Å in either buffer. Calcium ions bind to Stm and may serve as building blocks for calcium carbonate crystal formation, while other cations like Na^+ may regulate the further compaction of Stm, possibly accelerating or inhibiting the formation of PILP. Endolymph is the fluid present in the membranous labyrinth of the inner ear. It is a complex mixture, in which neither ions nor macromolecules are equally distributed. Moreover, the concentration of all molecules depends on the circadian rhythm, as otolith layers exhibit diurnal growth.[69,70] The relationship between endolymph composition and otolith formation is poorly understood at this time.

A possible explanation of the Ca^{2+}-dependent collapse of Stm/StmP molecules is that a negatively charged neighboring Asp or Glu formed bridging interactions between two or more carboxylic and/or phosphate groups and the calcium ions. The screening effect of sodium cations decreased this effect by electrostatic interactions with negatively charged residues. However, only a slight change in the secondary structure of Stm was observed under these conditions. A much stronger change was seen in the case of the RTX repeat domain (RD) of CyaA toxin from *Bordetella pertussis*.[72] However, in the presence of Ca^{2+}, a compaction of the RD with induction of the secondary structure was observed.

In conclusion, we believe that the intrinsically disordered character of Stm and the capability it has for calcium binding are essential for calcium carbonate biomineralization. Furthermore, phosphorylation affected Stm activity,[28] the protein structure, and Ca^{2+} binding.

AUTHOR INFORMATION

Corresponding Author

*E-mail: piotr.dobryszycki@pwr.edu.pl. Phone: +48713206332.

Funding

This research was financed by the National Science Center, Poland, via Grant NN 204 1200 40 (to P.D.), and in part by a statutory activity subsidy from the Polish Ministry of Science and High Education (S 40517) for the Faculty of Chemistry of Wrocław University of Technology.

Notes

The authors declare no competing financial interest.

ABBREVIATIONS

Stm, Starmaker; StmP, phosphorylated Starmaker; PILP, polymer-induced liquid precursor; PSer, phosphoserine; PThr, phosphothreonine; IDP, intrinsically disordered protein; DSP, dentin sialoprotein; DPP, dentin phosphoprotein; DSPP, dentin sialophosphoprotein; CK2, casein kinase 2; DMP-1, dentin matrix protein-1; BSP, bone sialoprotein; OPN, osteopontin; SIBLING, small integrin binding ligand, N-linked glycoprotein.

REFERENCES

(1) Feng, Q. (2011) Principles of Calcium-Based Biomineralization. In *Molecular Biomineralization* (Muller, W. E. G., Ed.) pp 141−197, Springer, Berlin.

(2) Skinner, H., and Jahren, A. (2007) Biomineralization. In *Biogeochemistry* (Schlesinger, W., Ed.) 2nd ed., pp 117−183, Elsevier-Pergamon, Oxford, U.K.

(3) Ross, M. D., and Pote, K. G. (1984) Some properties of otoconia. *Philos. Trans. R. Soc., B 304*, 445−452.

(4) Popper, A. N., Fay, R. R., Platt, C., and Sand, O. (2003) Sound Detection Mechanism and Capabilities of Teleost Fishes. In *Sensory Processing in Aquatic Environments* (Collin, S. P., and Marshall, J. N., Eds.) pp 3−38, Springer, New York.

(5) Boskey, A. L. (2003) Biomineralization: An overview. *Connect. Tissue Res. 44* (Suppl. 1), 5−9.

(6) Weiner, S. (2008) Biomineralization: A structural perspective. *J. Struct. Biol. 163*, 229−234.

(7) Gower, L. B. (2008) Biomimetic model systems for investigating the amorphous precursor pathway and its role in biomineralization. *Chem. Rev. 108*, 4551−4627.

(8) Marin, F., and Luquet, G. (2007) Unusually Acidic Proteins in Biomineralization. In *Handbook of Biomineralization* (Bäuerlein, E., Ed.) pp 273−290, Wiley-VCH Verlag GmbH, Weinheim, Germany.

(9) Gorski, J. P. (1992) Acidic phosphoproteins from bone matrix: A structural rationalization of their role in biomineralization. *Calcif. Tissue Int. 50*, 391−396.

(10) George, A., and Veis, A. (2008) Phosphorylated proteins and control over apatite nucleation, crystal growth, and inhibition. *Chem. Rev. 108*, 4670−4693.

(11) Jain, A., Karadag, A., Fohr, B., Fisher, L. W., and Fedarko, N. S. (2002) Three SIBLINGs (small integrin-binding ligand, N-linked glycoproteins) enhance factor H's cofactor activity enabling MCP-like cellular evasion of complement-mediated attack. *J. Biol. Chem. 277*, 13700−13708.

(12) Wojtas, M., Dobryszycki, P., and Ożyhar, A. (2012) Intrinsically Disordered Proteins in Biomineralization. In *Advanced Topics in Biomineralization* (Seto, J., Ed.) pp 3−32.

(13) Uversky, V. N., Gillespie, J. R., and Fink, A. L. (2000) Why are "natively unfolded" proteins unstructured under physiologic conditions? *Proteins: Struct., Funct., Genet. 41*, 415−427.

(14) Cross, K. J., Huq, N. L., and Reynolds, E. C. (2005) Protein dynamics of bovine dentin phosphophoryn. *J. Pept. Res. 66*, 59−67.

(15) Stetler-Stevenson, W. G., and Veis, A. (1987) Bovine dentin phosphophoryn: Calcium ion binding properties of a high molecular weight preparation. *Calcif. Tissue Int. 40*, 97−102.

(16) He, G., Ramachandran, A., Dahl, T., George, S., Schultz, D., Cookson, D., Veis, A., and George, A. (2005) Phosphorylation of phosphophoryn is crucial for its function as a mediator of biomineralization. *J. Biol. Chem. 280*, 33109−33114.

(17) Campbell, K. P., MacLennan, D. H., Jorgensen, A. O., and Mintzer, M. C. (1983) Purification and characterization of

DOI: 10.1021/acs.biochem.5b00933
Biochemistry 2015, 54, 6525−6534

calsequestrin from canine cardiac sarcoplasmic reticulum and identification of the 53,000 Da glycoprotein. *J. Biol. Chem. 258*, 1197−1204.
(18) Nelson, D. E., Glaunsinger, B., and Bohnert, H. J. (1997) Abundant accumulation of the calcium-binding molecular chaperone calreticulin in specific floral tissues of *Arabidopsis thaliana*. *Plant Physiol. 114*, 29−37.
(19) Li, X., Su, R. T., Hsu, H. T., and Sze, H. (1998) The molecular chaperone calnexin associates with the vacuolar H(+)-ATPase from oat seedlings. *Plant Cell 10*, 119−130.
(20) Heyen, B. J., Alsheikh, M. K., Smith, E. A., Torvik, C. F., Seals, D. F., and Randall, S. K. (2002) The calcium-binding activity of a vacuole-associated, dehydrin-like protein is regulated by phosphorylation. *Plant Physiol. 130*, 675−687.
(21) Dziedzic-Letka, A., Rymarczyk, G., Kapłon, T. M., Górecki, A., Szamborska-Gbur, A., Wojtas, M., Dobryszycki, P., and Ożyhar, A. (2011) Intrinsic disorder of *Drosophila melanogaster* hormone receptor 38 N-terminal domain. *Proteins: Struct., Funct., Genet. 79*, 376−392.
(22) Iakoucheva, L. M., Radivojac, P., Brown, C. J., O'Connor, T. R., Sikes, J. G., Obradovic, Z., and Dunker, A. K. (2004) The importance of intrinsic disorder for protein phosphorylation. *Nucleic Acids Res. 32*, 1037−1049.
(23) Fekete, D. M. (2003) Developmental biology. rocks that roll zebrafish. *Science 302*, 241−242.
(24) Sollner, C., Burghammer, M., Busch-Nentwich, E., Berger, J., Schwarz, H., Riekel, C., and Nicolson, T. (2003) Control of crystal size and lattice formation by starmaker in otolith biomineralization. *Science 302*, 282−286.
(25) MacDougall, M., Simmons, D., Luan, X., Nydegger, J., Feng, J., and Gu, T. T. (1997) Dentin phosphoprotein and dentin sialoprotein are cleavage products expressed from a single transcript coded by a gene on human chromosome 4: DENTIN PHOSPHOPROTEIN DNA SEQUENCE DETERMINATION. *J. Biol. Chem. 272*, 835−842.
(26) Kapłon, T. M., Michnik, A., Drzazga, Z., Richter, K., Kochman, M., and Ożyhar, A. (2009) The rod-shaped conformation of starmaker. *Biochim. Biophys. Acta, Proteins Proteomics 1794*, 1616−1624.
(27) Kapłon, T. M., Rymarczyk, G., Nocula-Ługowska, M., Jakób, M., Kochman, M., Lisowski, M., Szewczuk, Z., and Ożyhar, A. (2008) Starmaker exhibits properties of an intrinsically disordered protein. *Biomacromolecules 9*, 2118−2125.
(28) Wojtas, M., Wołcyrz, M., Ożyhar, A., and Dobryszycki, P. (2012) Phosphorylation of intrinsically disordered starmaker protein increases its ability to control the formation of calcium carbonate crystals. *Cryst. Growth Des. 12*, 158−168.
(29) Gower, L. B., and Odom, D. J. (2000) Deposition of calcium carbonate films by a polymer-induced liquid-precursor (PILP) process. *J. Cryst. Growth 210*, 719−734.
(30) Lowry, O. H., Rosebrough, N. J., Farr, A. L., and Randall, R. J. (1951) Protein measurement with the folin phenol reagent. *J. Biol. Chem. 193*, 265−275.
(31) Laemmli, U. K. (1970) Cleavage of structural proteins during the assembly of the head of bacteriophage T4. *Nature 227*, 680−685.
(32) Engel, J., Taylor, W., Paulsson, M., Sage, H., and Hogan, B. (1987) Calcium binding domains and calcium-induced conformational transition of SPARC/BM-40/osteonectin, an extracellular glycoprotein expressed in mineralized and nonmineralized tissues. *Biochemistry 26*, 6958−6965.
(33) McNamara, C. J., Perry, T. D., 4th, Bearce, K., Hernandez-Duque, G., and Mitchell, R. (2005) Measurement of limestone biodeterioration using the Ca2+ binding fluorochrome Rhod-5N. *J. Microbiol. Methods 61*, 245−250.
(34) Linse, S., Johansson, C., Brodin, P., Grundstroem, T., Drakenberg, T., and Forsen, S. (1991) Electrostatic contributions to the binding of Ca2+ in calbindin D9k. *Biochemistry 30*, 154−162.
(35) Wojtas, M., Kapłon, T. M., Dobryszycki, P., and Ożyhar, A. (2012) The Effect of Counter Ions on the Conformation of Intrinsically Disordered Proteins Studied by Size-Exclusion Chromatography. In *Methods in Molecular Biology* (Uversky, V. N., and Dunker, A. K., Eds.) pp 319−330, Springer, New York.
(36) Andrew, P. (1970) Estimation of molecular size and molecular weights of biological compounds by gel filtration. *Method Biochem Anal. 18*, 1−53.
(37) Uversky, V. N. (2002) What does it mean to be natively unfolded? *Eur. J. Biochem. 269*, 2−12.
(38) Laue, T. M., Shah, B. D., Ridgeway, T. M., and Pelletier, S. L. (1992) Computer-Aided Interpretation of Analytical Sedimentation Data for Proteins. In *Analytical Ultracentrifugation in Biochemistry and Polymer Science* (Harding, S. E., Rowe, A. J., and Horton, J. C., Eds.) pp 90−125, The Royal Society of Chemistry, Cambridge, U.K.
(39) Zhao, H., Ghirlando, R., Piszczek, G., Curth, U., Brautigam, C. A., and Schuck, P. (2013) Recorded scan times can limit the accuracy of sedimentation coefficients in analytical ultracentrifugation. *Anal. Biochem. 437*, 104−108.
(40) Schuck, P. (2000) Size-distribution analysis of macromolecules by sedimentation velocity ultracentrifugation and Lamm equation modeling. *Biophys. J. 78*, 1606−1619.
(41) Sreerama, N., and Woody, R. W. (2000) Estimation of protein secondary structure from circular dichroism spectra: Comparison of CONTIN, SELCON, and CDSSTR methods with an expanded reference set. *Anal. Biochem. 287*, 252−260.
(42) Veis, A., Sfeir, C., and Wu, C. B. (1997) Phosphorylation of the proteins of the extracellular matrix of mineralized tissues by casein kinase-like activity. *Crit. Rev. Oral Biol. Med. 8*, 360−379.
(43) Suzuki, Y., Yamaguchi, A., Ikeda, T., Kawase, T., Saito, S., and Mikuni-Takagaki, Y. (1998) In situ phosphorylation of bone and dentin proteins by the casein kinase II-like enzyme. *J. Dent. Res. 77*, 1799−1806.
(44) Takeda, H., Kawasaki, A., Takahashi, M., Yamada, A., and Koike, T. (2003) Matrix-assisted laser desorption/ionization time-of-flight mass spectrometry of phosphorylated compounds using a novel phosphate capture molecule. *Rapid Commun. Mass Spectrom. 17*, 2075−2081.
(45) Kinoshita, E., Kinoshita-Kikuta, E., Takiyama, K., and Koike, T. (2005) Phosphate-binding tag, a new tool to visualize phosphorylated proteins. *Mol. Cell. Proteomics 5*, 749−757.
(46) Chen, Y., Bal, B. S., and Gorski, J. P. (1992) Calcium and collagen binding properties of osteopontin, bone sialoprotein, and bone acidic glycoprotein-75 from bone. *J. Biol. Chem. 267*, 24871−24878.
(47) Endo, H., Takagi, Y., Ozaki, N., Kogure, T., and Watanabe, T. (2004) A crustacean Ca2+-binding protein with a glutamate-rich sequence promotes CaCO3 crystallization. *Biochem. J. 384*, 159−167.
(48) Siegel, L. M., and Monty, K. J. (1966) Determination of molecular weights and frictional ratios of proteins in impure systems by use of gel filtration and density gradient centrifugation. Application to crude preparations of sulfite and hydroxylamine reductases. *Biochim. Biophys. Acta, Biophys. Incl. Photosynth. 112*, 346−362.
(49) Tcherkasskaya, O., and Uversky, V. N. (2001) Denatured collapsed states in protein folding: Example of apomyoglobin. *Proteins: Struct., Funct., Genet. 44*, 244−254.
(50) Kelly, S. M., Jess, T. J., and Price, N. C. (2005) How to study proteins by circular dichroism. *Biochim. Biophys. Acta, Proteins Proteomics 1751*, 119−139.
(51) Qin, C., Baba, O., and Butler, W. T. (2004) Post-translational modifications of sibling proteins and their roles in osteogenesis and dentinogenesis. *Crit. Rev. Oral Biol. Med. 15*, 126−136.
(52) Ganss, B., Kim, R. H., and Sodek, J. (1999) Bone sialoprotein. *Crit. Rev. Oral Biol. Med. 10*, 79−98.
(53) Goldberg, H. A., and Hunter, G. K. (1995) The inhibitory activity of osteopontin on hydroxyapatite formation in vitro. *Ann. N. Y. Acad. Sci. 760*, 305−308.
(54) He, G., Dahl, T., Veis, A., and George, A. (2003) Nucleation of apatite crystals in vitro by self-assembled dentin matrix protein 1. *Nat. Mater. 2*, 552−558.
(55) Suzuki, S., Sreenath, T., Haruyama, N., Honeycutt, C., Terse, A., Cho, A., Kohler, T., Muller, R., Goldberg, M., and Kulkarni, A. B. (2009) Dentin sialoprotein and dentin phosphoprotein have distinct roles in dentin mineralization. *Matrix Biol. 28*, 221−229.

DOI: 10.1021/acs.biochem.5b00933
Biochemistry 2015, 54, 6525−6534

(56) Fujisawa, R., Mizuno, M., Nodasaka, Y., and Yoshinori, K. (1997) Attachment of osteoblastic cells to hydroxyapatite crystals by a synthetic peptide (Glu-Pro-Arg-Gly-Asp-Thr) containing two functional sequences of bone sialoprotein. *Matrix Biol. 16*, 21−28.
(57) Fujisawa, R., and Kuboki, Y. (1998) Conformation of dentin phosphophoryn adsorbed on hydroxyapatite crystals. *Eur. J. Oral Sci. 106* (Suppl. 1), 249−253.
(58) Kim, I. W., Morse, D. E., and Evans, J. S. (2004) Molecular characterization of the 30-AA N-terminal mineral interaction domain of the biomineralization protein AP7. *Langmuir 20*, 11664−11673.
(59) Michenfelder, M., Fu, G., Lawrence, C., Weaver, J. C., Wustman, B. A., Taranto, L., Evans, J. S., and Morse, D. E. (2003) Characterization of two molluscan crystal-modulating biomineralization proteins and identification of putative mineral binding domains. *Biopolymers 70*, 522−533.
(60) Zhang, B., Wustman, B. A., Morse, D., and Evans, J. S. (2002) Model peptide studies of sequence regions in the elastomeric biomineralization protein, lustrin A. I. the C-domain consensus-PG-, -NVNCT-motif. *Biopolymers 63*, 358−369.
(61) Wustman, B. A., Weaver, J. C., Morse, D. E., and Evans, J. S. (2003) Structure-function studies of the lustrin A polyelectrolyte domains, RKSY and D4. *Connect. Tissue Res. 44* (Suppl. 1), 10−15.
(62) Delak, K., Giocondi, J., Orme, C., and Evans, J. S. (2008) Modulation of crystal growth by the terminal sequences of the prismatic-associated asprich protein. *Cryst. Growth Des. 8*, 4481−4486.
(63) Inoue, H., Ohira, T., and Nagasawa, H. (2007) Significance of the N- and C-terminal regions of CAP-1, a cuticle calcification-associated peptide from the exoskeleton of the crayfish, for calcification. *Peptides 28*, 566−573.
(64) Gribble, F. M., Loussouarn, G., Tucker, S. J., Zhao, C., Nichols, C. G., and Ashcroft, F. M. (2000) A novel method for measurement of submembrane ATP concentration. *J. Biol. Chem. 275*, 30046−30049.
(65) Thompson, R. J., Akana, H. C. S. R., Finnigan, C., Howell, K. E., and Caldwell, J. H. (2005) Anion channels transport ATP into the Golgi lumen. *American Journal of Physiology - Cell Physiology 290*, C499−C514.
(66) Grankowski, N., Boldyreff, B., and Issinger, O. G. (1991) Isolation and characterization of recombinant human casein kinase II subunits alpha and beta from bacteria. *Eur. J. Biochem. 198*, 25−30.
(67) Sanchez, E. J., Munske, G. R., Criswell, A., Milting, H., Dunker, A. K., and Kang, C. (2011) Phosphorylation of human calsequestrin: Implications for calcium regulation. *Mol. Cell. Biochem. 353*, 195−204.
(68) Donato, R. (2001) S100: A multigenic family of calcium-modulated proteins of the EF-hand type with intracellular and extracellular functional roles. *Int. J. Biochem. Cell Biol. 33*, 637−668.
(69) Payan, P., Edeyer, A., de Pontual, H., Borelli, G., Boeuf, G., and Mayer-Gostan, N. (1999) Chemical composition of saccular endolymph and otolith in fish inner ear: Lack of spatial uniformity. *Am. J. Physiol. 277*, R123−31.
(70) Borelli, G., Mayer-Gostan, N., De Pontual, H., Boeuf, G., and Payan, P. (2001) Biochemical relationships between endolymph and otolith matrix in the trout (*Oncorhynchus mykiss*) and turbot (*Psetta maxima*). *Calcif. Tissue Int. 69*, 356−364.
(71) Dai, L., Cheng, X., and Gower, L. B. (2008) Transition bars during transformation of an amorphous calcium carbonate precursor. *Chem. Mater. 20*, 6917−6928.
(72) Chenal, A., Guijarro, J. I., Raynal, B., Delepierre, M., and Ladant, D. (2008) RTX calcium binding motifs are intrinsically disordered in the absence of calcium: Implication for protein secretion. *J. Biol. Chem. 284*, 1781−1789.

DOI: 10.1021/acs.biochem.5b00933
Biochemistry 2015, 54, 6525−6534